Letters

A Versatile Resonant Tank Identification Methodology for Induction Heating Systems

Héctor Sarnago, *Member, IEEE*, Oscar Lucía, *Senior Member, IEEE*, and Jose M. Burdio, *Senior Member, IEEE*

***Abstract*—Induction heating has become the most advance heating process due to benefits, such as efficiency, performance, cleanness, and safety. In this process, the electromagnetic coupling between the induction coil and the induction target is a key, determining the heating performance as well as the resonant power converter operation. This letter proposes an accurate and cost-effective resonant tank identification method applied to induction heating systems. It is based on monitoring the resonant capacitor voltage in order to calculate the resonant tank quality factor. The proposed methodology has been tested using a versatile power electronics test bench applied to domestic induction heating, proving the feasibility of this proposal.**

***Index Terms*—Home appliances, induction heating (IH), inverters, resonant power conversion.**

Introduction

Induction heating (IH) has become the heating technology of choice in many industrial [1], domestic [2], and medical applications [3] due to its benefits in terms of efficiency cleanliness and performance, leading to a superior quality process [4]. Regardless the application, IH is based on applying an alternating magnetic field to an induction target to be heated. Consequently, the main heating mechanism in industrial and domestic applications relies on the induced *Eddy currents* which heats the induction target by the *Joule* effect. In this phenomenon, as it occurs in most wireless power transfer systems [5], the electromagnetic coupling between the induction coil and the induction target is essential (see Fig. 1), since it determines the IH process as well as the power converter operating point. It depends strongly on the geometry and relative position of the elements, the excitation frequency, temperature, and materials, among other factors.

Manuscript received May 30, 2017; revised July 15, 2017; accepted August 5, 2017. Date of publication August 17, 2017; date of current version December 1, 2017. This work was supported in part by the Spanish MINECO under Project TEC2016-78358-R and Project RTC-2014-1847-6, in part by the DGA-FSE, and in part by the BSH Home Appliances Group. *(Corresponding author: Oscar Lucía.)*

The authors are with the University of Zaragoza, Zaragoza 50018, Spain (e-mail: hsarnago@unizar.es; olucia@unizar.es; burdio@unizar.es).

Color versions of one or more of the figures in this letter are available online at http://ieeexplore.ieee.org.

Digital Object Identifier 10.1109/TPEL.2017.2740998

Fig. 1. IH coils with different electromagnetic coupling ratio to the IH target.

Most modern IH systems rely on the use of resonant power converters due to its advantages in terms of efficiency and performance due to the soft-switching operation and low harmonic emissions. Thus, the IH load is a part of the resonant tank and, consequently, severely affects the power converter operation and its performance. Therefore, an accurate identification of the main IH target characteristics is essential to ensure not only the proper system performance but also to ensure is reliability [6], [7].

The aim of this letter is to propose an accurate and cost-effective resonant tank identification system applied to an IH system. The proposed system relies on measuring the resonant capacitor voltage in order to calculate the resonant tank quality factor, providing useful information about the electromagnetic coupling. This enables to detect the presence of an IH load as well as the coverage ratio in order to optimize the heating process by adapting the control algorithm to changes in the plant [6] or adapt the output power of partly covered coils to optimize the heat distribution in the pot. Besides, the proposed measurement technique avoids the need for commonly used costly and bulky current transformers. The remainder of this letter is organized as follows. Section II details the proposed IH load detection system, including the resonant power converter, calculation methodology, and digital implementation. Section III summarizes the main implementation and experimental results performed with a versatile power electronics test bench and dif-

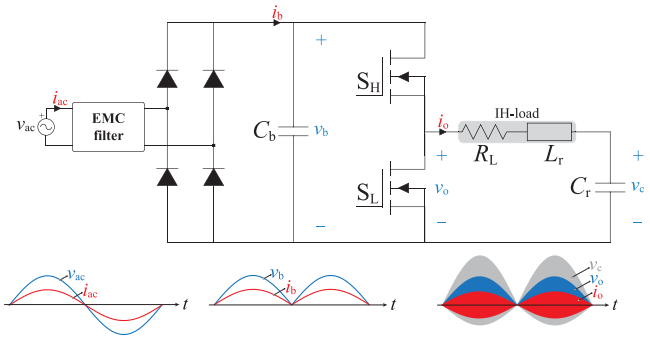

Fig. 2. Half-bridge series-resonant inverter: Schematic and main waveforms.

ferent operating conditions. Finally, Section IV draws the main conclusions of this letter.

II. Proposed IH Load Detection System

A. Resonant Power Converter

Modern IH systems are based on resonant power converters due to their benefits in terms of performance and efficiency. Among the available resonant topologies [4], [8]–[10], the class-D topologies [11] are generally preferred due to their balanced performance operation and cost. Fig. 2(a) shows the schematic of the half-bridge series-resonant converter, which is commonly applied to domestic IH. It is composed of two unipolar bidirectional devices, commonly IGBTs with antiparallel diodes and the resonant tank. The resonant tank is composed of the IH target, modeled as the series connection of a resistor R_L and an inductor L_r, and the resonant capacitor C_r [12]. When the IH load changes, i.e., geometry, coupling, materials, or temperature, both R_L and L_r are modified.

In order to quantify the IH load change, the quality factor, as defined later, is preferred because it is approximately constant in the operating range and offers useful information about the IH load [13], enabling to design accurate converter control and safe operating conditions [6]. Fig. 2(b) shows the main waveforms including the control signals, output voltage and current, and resonant capacitor voltage. The series-resonant half-bridge inverter is usually designed to operate above the resonant frequency to achieve zero-voltage switching, and the output power is controlled by increasing the switching frequency.

B. Identification Method

The proposed detection method is based on analyzing the changes in the resonant network previously detailed. For a series-resonant inverter, the resonant frequency ω_o is defined as

$$\omega_o = \frac{1}{\sqrt{L_r C_r}}. \tag{1}$$

The quality factor Q is a dimensionless parameter that characterizes the circuit bandwidth and which enables to accurately detect the main features of the IH target. In this circuit, it can be defined at a given switching frequency $\omega_{\rm sw}$ as

$$Q_{\rm sw} = \frac{\omega_{\rm sw} L_r}{R_L}. \tag{2}$$

In order to calculate the electrical equivalent parameters, several methods have been proposed in the past, including frequency-domain approaches [14], dedicated test benches [15], and output-power characterization [16]. However, these approaches require often several measurements as well as complex postprocessing requiring intensive computing power. The proposed approach calculates the quality factor by measuring only the resonant capacitor voltage, which can be performed using cost-effective passive elements and ADCs.

Considering as initial point (2), the equivalent IH load resistance can be calculated using

$$R_L = \frac{P_o}{I_{o,\rm rms}^2} \tag{3}$$

where $I_{o,\rm rms}$ is the RMS inverter output current. Considering the series-resonant tank and steady state assuming $T_{\rm sw} \ll T_{\rm ac}$, the output current can be calculated using partial integration as follows:

$$\begin{aligned} I_{o,\rm rms}^2 &= \frac{1}{T_{\rm sw}} \int_{T_{\rm sw}} i_o^2 dt \\ &= \frac{1}{T_{\rm sw}} \, i_o|_0^{T_{\rm sw}} \underbrace{\int_{T_{\rm sw}} i_o dt}_{I_c = 0} - \frac{1}{T_{\rm sw}} \int_{T_{\rm sw}} \left(\frac{di_o}{dt}\right) \left(\int i_o dt\right) dt \end{aligned} \tag{4}$$

where the integral part can be expressed as a function of the circuit voltages and the resonant elements using the following expression:

$$\begin{aligned} I_{o,\rm rms}^2 &= -\frac{1}{T_{\rm sw}} \int_{T_{\rm sw}} \left(\underbrace{\frac{di_o}{dt}}_{1/\,L_r\, v_L\,(t)} \right) \left(\underbrace{\int i_o dt}_{C_r\, v_c\,(t)} \right) dt \\ &= -\frac{C_r}{L_r} \frac{1}{T_{\rm sw}} \int_{T_{sw}} v_c \,(v_o - v_c - R_L i_o) dt. \end{aligned} \tag{5}$$

Finally, by analyzing each one of the integral terms, this expression can be simplified to be only a function of the resonant capacitor voltage and the dc-link voltage V_s

$$\begin{aligned} I_{o,\rm rms}^2 &= -\frac{C_r}{L_r} \frac{1}{T_{\rm sw}} \left(\int_{T_{\rm sw}} v_c v_o dt - \underbrace{\int_{T_{\rm sw}} v_c v_c dt}_{T_{\rm sw} V_{c,\rm rms}^2} \right. \\ &\quad \left. - R_L \underbrace{\int_{T_{\rm sw}} v_c i_o dt}_{E_c = 0} \right) \\ &= \frac{C_r}{L_r} \left(V_{c,\rm rms}^2 - \frac{V_s}{T_{\rm sw}} \int_0^{DT_{sw}} v_c(t) dt \right). \end{aligned} \tag{6}$$

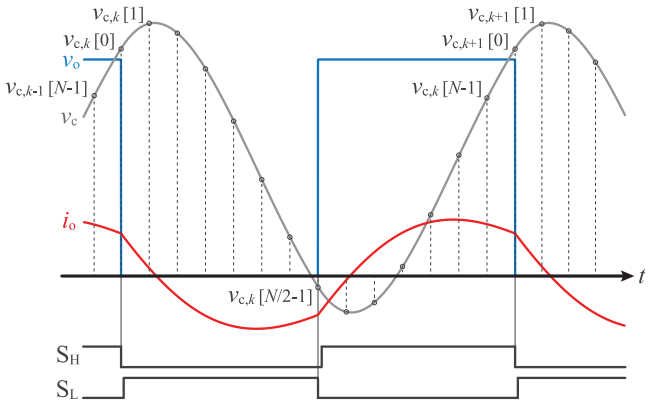

Fig. 3. Resonant converter main waveforms and sampling points.

Consequently, combining (3) and (6) in (2), the quality factor can be calculated as a function of the resonant capacitor voltage and the output power

$$Q_{\rm sw} = \frac{\omega_{\rm sw} L_r I_{o,\rm rms}^2}{P_o} = \frac{\omega_{\rm sw} C_r \left(V_{c,\rm rms}^2 - \frac{V_s}{T_{\rm sw}} \int_0^{DT_{\rm sw}} v_c(t)dt\right)}{P_o}. \tag{7}$$

Finally, by expressing the output power as a function of the resonant capacitor voltage [17]:

$$P_o = f_{\rm sw} C_r V_s \left(v_c(t=0) - v_c(t=DT_{\rm sw})\right) \tag{8}$$

and assuming a square-wave modulation, i.e., $D = 0.5$, $V_s = (v_c(t=0) + v_c(t=DT_{\rm sw}))$, the previous equation can be rewritten in a form depending only on v_c as follows:

$$Q_{\rm sw} = \frac{\omega_{\rm sw} C_r \left(V_{c,\rm rms}^2 - \frac{V_s}{T_{\rm sw}} \int_0^{DT_{\rm sw}} v_c(t)dt\right)}{P_o}$$

$$= \frac{2\pi(V_{c,\rm rms}^2 - (v_c(t=0) + v_c(t=DT_{\rm sw}))(\frac{1}{T_{\rm sw}} \int_0^{DT_{\rm sw}} v_c(t)dt))}{(v_c(t=0) + v_c(t=DT_{\rm sw}))(v_c(t=0) - v_c(t=DT_{\rm sw}))} \tag{9}$$

where $v_c(t=0)$ and $v_c(t=DT_{\rm sw})$ are the values of the resonant capacitor voltage at the turn-off transitions of S_H and S_L, respectively.

C. Digital implementation

In order to provide a suitable approach for digital implementation, the resonant capacitor voltage must be measured and equation discretized. The resonant capacitor voltage is sampled using a resistor voltage divider as shown in Fig. 3, where a switching period k with N samples is represented. It is important to note that the points $v_{c,k}[0]$ and $v_{c,k}[N/2-1]$ are key to calculate the output power and, consequently, the quality factor.

Expression (9) can be discretized to be calculated as follows:

$$Q_{{\rm sw},k} = \frac{2\pi}{N} \times \left(\frac{\sum_{n=0}^{N-1} v_{c,k}^2[n] - (v_{c,k}[0] + v_{c,k}[N/2-1]) \sum_{n=0}^{N/2-1} v_{c,k}[n]}{v_{c,k}^2[0] - v_{c,k}^2[N/2-1]}\right). \tag{10}$$

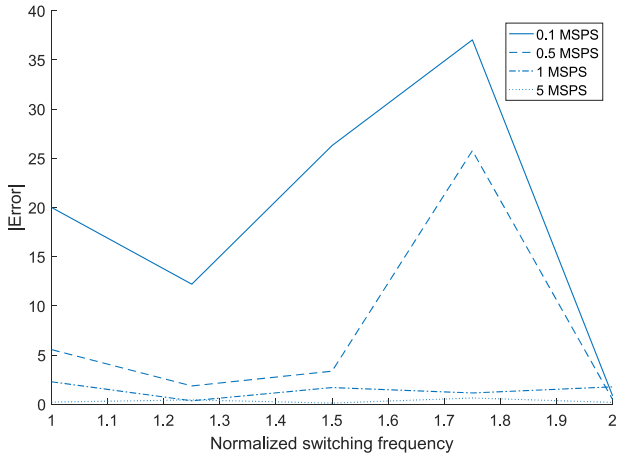

Fig. 4. Quality factor estimation error versus sampling rate for different sampling rates.

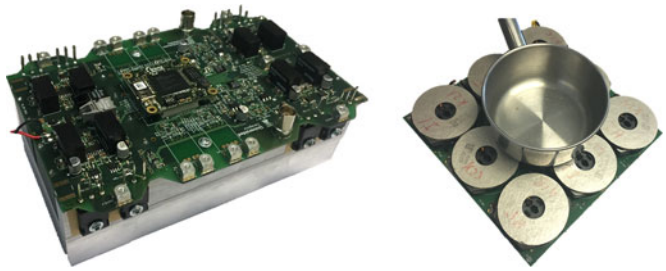

Fig. 5. Experimental test bench including power converter and induction target.

Finally, the average quality factor over a mains period $T_{\rm ac} = 1/f_{\rm ac}$ results $Q_{\rm sw,avg} = \frac{1}{K}\sum_{k=0}^{K-1} Q_{{\rm sw},k}$, where K denotes the number of switching periods during a mains period $K = f_{\rm sw}/f_{\rm ac}$. It is important to note that this expression depends only on the resonant capacitor voltage, providing a versatile and cost-effective method to estimate the IH load through its quality factor.

There are two main elements to be considered when analyzing the accuracy of the proposed method. The first one is the tolerance in the resonant capacitor value, which must be typically calibrated for each batch during the production process. The second one implies the optimization of the tradeoff between cost and error in the selection of the ADC sampling rate. Fig. 4 shows the error versus sampling rate for a typical IH load ($R_L = 12\,\Omega$, $L_r = 180\,\mu H$, and $C_r = 78$ nF). From this figure, it is clear that errors below the 5% can be obtained in the entire operation range.

III. Experimental Results

In order to prove the feasibility of the proposed identification system, a versatile power converter has been designed and implemented (see Fig. 5). It is a MOSFET-based implementation enabling the implementation of four half-bridge branches which are controlled using a versatile field-programmable gate array (FPGA)-based control architecture. The resonant capacitor

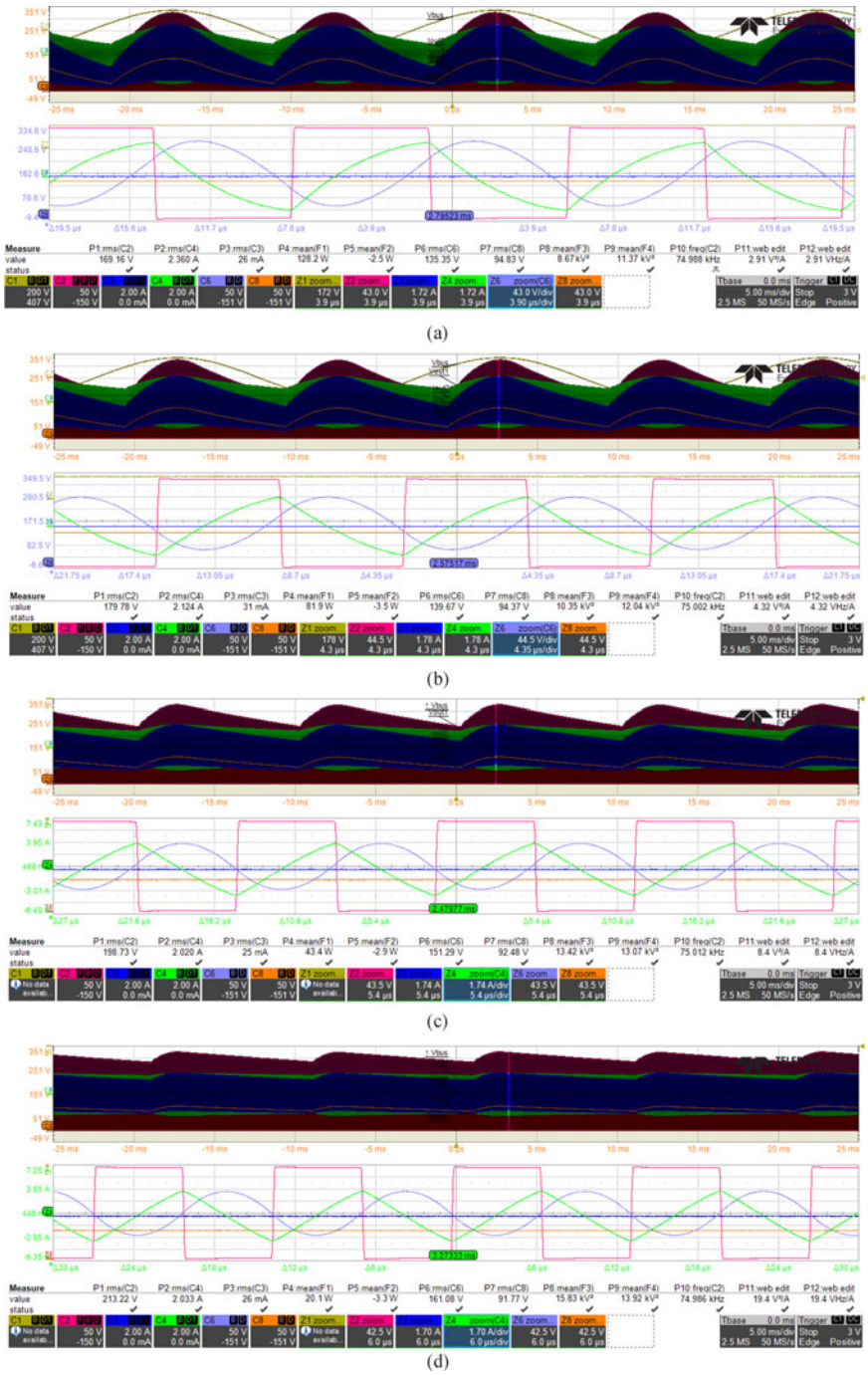

Fig. 6. Main experimental waveforms for different coverage ratios: (a) Fully covered $Q_{\mathrm{sw}} = 2.91$, (b) partially covered $Q_{\mathrm{sw}} = 4.32$, (c) partially covered $Q_{\mathrm{sw}} = 8.4$, and (d) slightly covered $Q_{\mathrm{sw}} = 19.4$. From top to bottom: Output voltage (50 V/div), output current (2 A/div), and resonant capacitor voltage (50 V/div).

voltage is measured using inexpensive voltage-divider resistors and 1-MSPS 10-bit ADC converter.

Fig. 6 shows the main experimental waveforms including the output voltage, current, and resonant capacitor voltage for an IH load with different coverage ratios, i.e., electromagnetic coupling. In this figure, the changes in bus voltage and coil current under different coverage ration can be seen. Besides, it can be clearly seen that the measurement of the resonant capacitor voltage, which contains lower harmonic content, provides an straight-forward implementation. The variation in the resonant capacitor voltage evaluated using (7) enables calculating the quality factor in order to estimate the IH load.

In Fig. 7, the error results comparing the proposed implementation and the results obtained using a LeCroy HDO8000 12-bit digital oscilloscope have been added for the same operation points, as shown in Fig. 6. These results prove experimentally the accuracy of the proposed implementation.

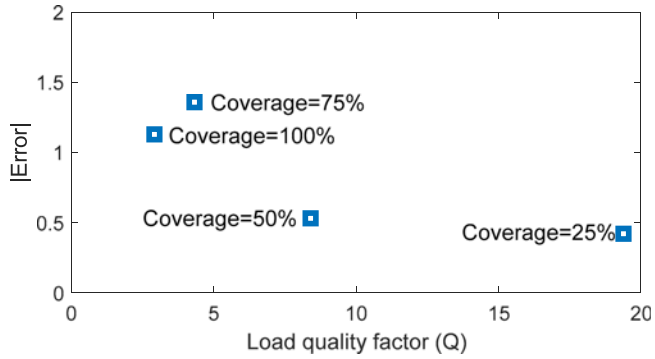

Fig. 7. Measured error as a function of the quality factor position.

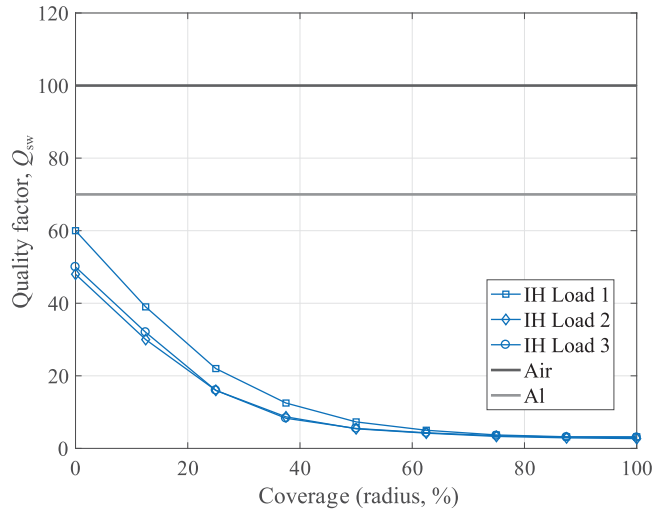

Fig. 8. Quality factor as a function of the coverage percent for different IH loads, aluminum, and air.

Finally, Fig. 8 summarizes the experimentally calculated quality factors Q_{sw} using the detailed test bench for different materials, including aluminum pots and air, and different coverage rations. Different materials, i.e., IH load 1–3, have been tested using 8-cm inductors and different coverage radii, as shown in Fig. 5. It is important to remark that the proposed technique enables to distinguish materials not to be heated, i.e., aluminum or air, from working materials and, more importantly, the coverage ratio in order to adapt the output power to improve the heating process. Parameters enable to optimize the power converter operation, optimizing its reliability and performance. Besides, the proposed technique is based on measuring the resonant capacitor voltage, avoiding the need of expensive and bulky current transformers, which limits the current state-of-the-art implementations.

IV. Conclusion

In this letter, an accurate and cost-effective method for detecting IH loads has been proposed and experimentally verified. It relies on the calculating of the quality factor of the resonant tank using a simplified approach measuring the resonant capacitor voltage, enabling an efficient implementation. The proposed methodology enables detecting the presence of an IH load as well as estimating the coverage percentage without the need of costly and bulky current sensors. This approach provides a versatile implementation which enables the optimization of IH and wireless power transfer systems relying on resonant networks.

References

[1] V. Esteve *et al.*, "Improving the reliability of series resonant inverters for induction heating applications," *IEEE Trans. Ind. Electron.*, vol. 61, no. 5, pp. 2564–2572, May 2014.

[2] O. Lucía, J. Acero, C. Carretero, and J. M. Burdío, "Induction heating appliances: Towards more flexible cooking surfaces," *IEEE Ind. Electron. Mag.*, vol. 7, no. 3, pp. 35–47, Sep. 2013.

[3] P. Di Barba, F. Dughiero, E. Sieni, and A. Candeo, "Coupled field synthesis in magnetic fluid hyperthermia," *IEEE Trans. Magn.*, vol. 47, no. 5, pp. 914–917, May 2011.

[4] O. Lucía, P. Maussion, E. Dede, and J. M. Burdío, "Induction heating technology and its applications: Past developments, current technology, and future challenges," *IEEE Trans. Ind. Electron.*, vol. 61, no. 5, pp. 2509–2520, May 2014.

[5] Y. Jian, L. Deyan, L. Chi-Kwan, and S. Y. R. Hui, "A systematic approach for load monitoring and power control in wireless power transfer systems without any direct output measurement," *IEEE Trans. Power Electron.*, vol. 30, no. 3, pp. 1657–1667, Mar. 2015.

[6] O. Jiménez, O. Lucia, I. Urriza, L. A. Barragán, P. Mattavelli, and D. Boroyevich, "FPGA-based gain-scheduled controller for resonant converters applied to induction cooktops," *IEEE Trans. Power Electron.*, vol. 29, no. 4, pp. 2143–2152, Apr. 2014.

[7] A. M. Stankovic, D. J. Perreault, and K. Sato, "Synthesis of dissipative nonlinear controllers for series resonant DC/DC converters," *IEEE Trans. Power Electron.*, vol. 14, no. 4, pp. 673–682, Jul. 1999.

[8] M. K. Kazimierczuk and D. Czarkowski, *Resonant Power Converters*. New York, NY, USA: Willey, 2011.

[9] C. Bi, H. Lu, K. Jia, J. Hu, and H. Li, "A novel multiple-frequency resonant inverter for induction heating applications," *IEEE Trans. Power Electron.*, vol. 31, no. 12, pp. 8162–8171, Dec. 2016.

[10] T. Mishima, Y. Nakagawa, and M. Nakaoka, "A bridgeless BHB ZVS-PWM AC-AC converter for high-frequency induction heating applications," *IEEE Trans. Ind. Appl.*, vol. 51, no. 4, pp. 3304–3315, Jul./Aug. 2015.

[11] H. Sarnago, O. Lucía, A. Mediano, and J. M. Burdío, "Analytical model of the half-bridge series resonant inverter for improved power conversion efficiency and performance," *IEEE Trans. Power Electron.*, vol. 30, no. 8, pp. 4128–4143, Aug. 2015.

[12] C. Carretero, J. Acero, R. Alonso, J. M. Burdio, and F. Monterde, "Embedded ring-type inductors modeling with application to induction heating systems," *IEEE Trans. Magn.*, vol. 45, no. 12, pp. 5333–5343, Dec. 2009.

[13] J. Acero, R. Alonso, J. M. Burdio, L. A. Barragan, and D. Puyal, "Analytical equivalent impedance for a planar circular induction heating system," *IEEE Trans. Magn.*, vol. 42, no. 1, pp. 84–86, Jan. 2006.

[14] O. Jiménez, O. Lucía, I. Urriza, L. A. Barragán, and D. Navarro, "Analysis and implementation of FPGA-based online parametric identification algorithms for resonant power converters," *IEEE Trans. Ind. Informat.*, vol. 10, no. 2, pp. 1144–1153, May 2014.

[15] D. Puyal, C. Bernal, J. M. Burdío, J. Acero, and I. Millán, "Versatile high-frequency inverter module for large-signal inductive loads characterization up to 1.5 MHz and 7 kW," *IEEE Trans. Power Electron.*, vol. 23, no. 1, pp. 75–87, Jan. 2008.

[16] N. Domingo, L. A. Barragán, J. M. M. Montiel, A. Domínguez, and J. I. Artigas, "Fast power–frequency function estimation for induction heating appliances," *Electron. Lett.*, vol. 53, pp. 498–500, 2017.

[17] H. Sarnago, O. Lucía, D. Navarro, and J. M. Burdío, "Operating conditions monitoring for high power density and cost-effective resonant power converters," *IEEE Trans. Power Electron.*, vol. 31, no. 1, pp. 488–496, Jan. 2016.